ACI STRUCTURAL JOURNAL TECHNICAL PAPER

Title no. 102-S62

Bond Strength of Lap-Spliced Bars

by Erdem Canbay and Robert J. Frosch

Calculation methods to evaluate the strength of tension lap splices are based primarily on nonlinear regression analysis of test results. While the results from these analyses are extremely useful, applicability of their results beyond the domain of the data is often questioned. The objective of this research was to develop an expression for the calculation of bond strength based on a physical model of tension cracking of concrete in the lap-spliced region. Two different types of failure modes are considered: horizontal splitting that develops at the level of the bars (side-splitting failure), and vertical splitting that develops along the bar on the face cover (face-splitting failure). The developed expression was verified using results from 203 unconfined and 278 confined beam tests where the splice region was subjected to constant moment.

Keywords: bond; reinforced concrete; splice; stirrup.

INTRODUCTION

Because the performance of reinforced concrete structures depends on adequate bond strength between concrete and reinforcing steel, accurate calculation of splice strength is important. The ACI 318-02 (ACI Committee 318 2002) equation for development and splices of reinforcement is based on the expression for development length previously endorsed by ACI Committee 408 in ACI 408.1R-90 (ACI Committee 440 1990; Jirsa, Lutz, and Gergely 1979). This design expression is based on nonlinear regression analysis of test results available at the time. Since then, additional studies have been conducted that have investigated the behavior of lapped splices. With the increase of test data, new attempts have been made to better estimate splice strength based on statistical approaches incorporating the most recent data. To calculate bond strength more accurately, recent studies have included additional variables beyond those considered by ACI 318. Unfortunately, as more variables are added, the descriptive equations become more complex and cumbersome, especially for design applications.

RESEARCH SIGNIFICANCE

Although many studies on lap-spliced bars exist, a theory-based analysis procedure has not been developed. While additional test data have resulted in an increase in the accuracy of current statistical approaches, splice strength behavior remains not fully understood. Furthermore, the applicability of statistical approaches outside the domain of the data is often questioned. The objective of this study was to develop an expression for the calculation of bond strength based on a physical model of tension cracking of concrete in the lap-spliced region.

DESCRIPTIVE EQUATIONS

Two of the most commonly used modeling approaches have been provided by Orangun, Jirsa, and Breen (1977) and Zuo and Darwin (2000). These approaches are summarized in the following.

Orangun, Jirsa, and Breen (1977) developed an expression for calculating the development and splice lengths for deformed bars, as given in Eq. (1). This expression is based on a nonlinear regression analysis of test results of beams with lap splices and reflects the effect of length, cover, spacing, bar diameter, concrete strength, and transverse reinforcement on the strength of anchored bars. It is significant to note that this expression forms the basis for the bond requirements of the current ACI 318 Building Code

$$\frac{u}{\sqrt{f_c'}} = 1.2 + \frac{3C}{d_b} + \frac{50d_b}{\ell_s} + \frac{A_{tr}f_{yt}}{500sd_b} \quad (1)$$

where A_{tr} = area of transverse reinforcement normal to the plane of splitting through the anchored bars, in.^{2}; C = the smaller of c_b or c_s, in.; c_b = bottom clear cover of reinforcing bars, in.; c_s = half clear spacing between bars or splices or half available concrete width per bar or splice resisting splitting in the failure plane, in.; d_b = diameter of reinforcing bars, in.; f_c' = specified compressive strength of concrete, psi; f_{yt} = yield strength of transverse reinforcement, psi; ℓ_s = splice length, in.; s = spacing of transverse reinforcement, in.; and u = average bond stress, psi.

Zuo and Darwin (2000) evaluated the effects of concrete strength, coarse aggregate quantity and type, and reinforcing bar geometry on splice strength. They proposed a new expression that represents the development/splice strength of bottom-cast uncoated bars as a function of member geometry, concrete strength, relative rib area, bar size, and confinement provided by both concrete and transverse reinforcement. This expression is based on regression analysis and fits the data well for both unconfined and confined test data. It is significant to note that this expression forms the basis for the bond recommendations of ACI Committee 408 (2003). The Zuo and Darwin expression for confined specimens is given as follows

$$\frac{A_b f_s}{f_c'^{1/4}} = [59.8\ell_s(c_{min} + 0.5d_b) + 2350A_b] \quad (2)$$

$$\left(0.1\frac{c_{max}}{c_{min}} + 0.9\right) + \left(31.14t_r t_d \frac{NA_{tr}}{n} + 3.99\right)f_c'^{1/2}$$

where A_b = single spliced bar area, in.^{2}; c_{min}, c_{max} = minimum or maximum value of c_s or c_b; $c_s = min(c_{si} + 0.25, c_{so})$;

ACI Structural Journal, V. 102, No. 4, July-August 2005.
MS No. 04-178 received June 11, 2004, and reviewed under Institute publication policies.

Erdem Canbay *is an assistant professor of civil engineering at the Middle East Technical University, Ankara, Turkey. He received his BS from Istanbul Technical University, Istanbul, Turkey, and his MS and PhD from Middle East Technical University.*

Robert J. Frosch, *FACI, is an associate professor of civil engineering at Purdue University, West Lafayette, Ind. He received his BSE from Tulane University, New Orleans, La., and his MSE and PhD from the University of Texas at Austin, Austin, Tex. He is Chair of ACI Committee 224, Cracking, and is a member of ACI Committees 318, Structural Concrete Building Code; 408, Bond and Development of Reinforcement; and Joint ACI-ASCE Committee 445, Shear and Torsion.*

c_{so} = clear side cover of reinforcing bars, in.; c_{si} = half of the clear spacing between bars, in.; N = the number of transverse stirrups within the development or splice length; n = number of bars being developed or spliced; and R_r = relative rib area of reinforcement; $t_r = 9.6\,R_r + 0.28$; and $t_d = 0.78d_b + 0.22$.

BOND BEHAVIOR

As one of the main objectives of this study was to understand bond behavior and to develop an expression with a strong theoretical basis, a comprehensive literature survey was conducted. In particular, the survey concentrated on test results from beam tests containing lap splices located in a constant moment region. Pullout tests, tests with varying moment or shear over the splice region, and beam-end tests were excluded from this data set because, as noted by ACI Committee 408 (2003), these tests are difficult to interpret and can provide unconservative estimates of bond strength.

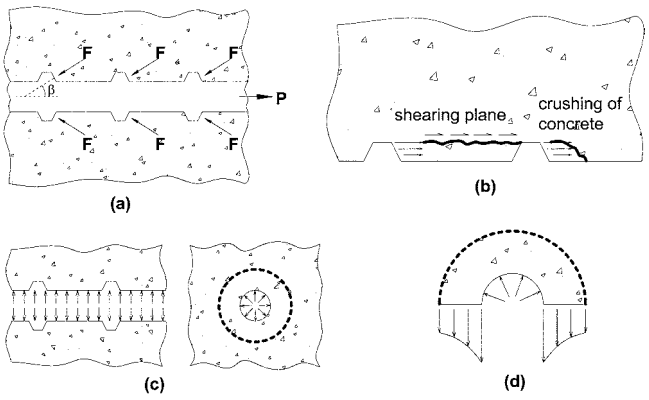

Fig. 1—Forces on concrete exerted by deformed reinforcing bars.

In total, 203 unconfined and 278 confined beam tests were obtained from the available literature complying with the aforementioned considerations. It should be noted that the database includes results only from specimens failing in splitting. The references and the range of the main variables are listed in Table 1 and 2 for unconfined and confined test data, respectively. In these tables, the concrete cover c is defined as the clear cover of concrete or half the clear spacing between spliced bars. In general, this database is consistent with the ACI 408 Database 10-2001 (ACI Committee 408 2003).

FAILURE MODES

When a deformed bar is exposed to tension, its lugs bear on the surrounding concrete. As shown in Fig. 1(a), the resultant force exerted by the lug on the concrete is inclined at an angle β to the axis of the bar (Goto 1971; Ferguson and Briceno 1969). While the component of this inclined force parallel to the bar axis causes shearing of the concrete between the lugs (Fig. 1(b)), the perpendicular component of this force exerts a radial force on the surrounding concrete (Fig. 1(c)). If the lugs are spaced far enough apart, pullout failure due to shearing of concrete between lugs does not occur. The radial forces cause concrete to act as a thick wall pipe subjected to internal pressure (Tepfers 1979, 1982). This pressure causes tensile forces on the surrounding pipe or concrete for this case as shown in Fig. 1(d). Splitting cracks in concrete occur if these tensile forces exceed the tension capacity of concrete.

For a splitting failure mode, the tensile strength of concrete surrounding the bar is a major parameter that affects the development of the reinforcement (DeVries, Moehle, and Hester 1991). In this study, two different splitting

Table 1—References for unconfined uncoated splice test data

Reference	Number of tests	Splice length ℓ_s, in.	Bar diameter d_b, in.	Concrete compressive strength f'_c, ksi	Concrete cover c, in.
Chinn, Ferguson, and Thompson (1955)	32	5.5 to 24.0	0.375 to 0.750	3.16 to 7.48	0.50 to 2.94
Chamberlin (1958)	2	6.0	0.500	4.37 to 4.45	0.50 to 2.50
Ferguson and Breen (1965)	26	18.0 to 82.5	1.000 to 1.410	2.61 to 4.65	1.31 to 4.70
Ferguson and Krishnaswamy (1971)	4	15.0 to 98.0	0.625 to 2.257	2.71 to 3.22	0.83 to 4.61
Thompson et al. (1975)	11	12.0 to 60.0	0.750 to 1.693	2.87 to 4.71	2.00 to 4.00
Treece and Jirsa (1989)	2	18.0 to 36.0	1.410	4.29 to 9.60	2.00 to 2.01
Cleary and Ramirez (1991)	4	10.0 to 16.0	0.750	3.99 to 8.20	2.00 to 3.25
Choi et al. (1991)	8	12.0 to 24.0	0.625 to 1.410	5.36 to 6.01	1.00 to 2.00
Hester et al. (1993)	7	16.0 to 22.8	1.000	5.24 to 6.45	1.50 to 4.00
Rezansoff, Akanni, and Sparling (1993)	4	29.5 to 44.3	0.990 to 1.180	3.73 to 4.03	0.99 to 2.01
Azizinamini et al. (1993)	13	13.0 to 80.0	1.000 to 1.410	5.08 to 15.12	1.00 to 1.81
Hwang, Lee, and Lee, (1994)	4	11.8	1.130	9.24 to 12.18	1.13 to 1.14
Darwin et al. (1996)	12	16.0 to 40.0	0.625 to 1.410	3.83 to 5.25	1.02 to 3.06
Hamad and Mansour (1996)	3	11.8 to 13.8	0.551 to 0.787	2.90 to 3.35	0.79 to 4.69
Hamad and Itani (1998)	8	12.0	0.984	7.59 to 11.12	1.50 to 1.58
Hamad and Machaka (1999)	3	12.0	0.984	6.77 to 13.46	1.02 to 1.10
Azizinamini et al. (1999)	32	10.0 to 80.0	1.000 to 1.410	5.08 to 15.59	1.00 to 3.36
Zuo and Darwin (2000)	28	16.5 to 40.0	0.625 to 1.410	4.25 to 15.65	0.51 to 4.05
Total	**203**	**5.5 to 98.0**	**0.375 to 2.257**	**2.61 to 15.65**	**0.50 to 4.70**

failure planes are assumed. Side splitting occurs when a horizontal split develops at the level of bars as shown in Fig. 2(a). Face splitting occurs when a vertical split develops below the bars. For the sake of simplicity, it is assumed that a cracking plane develops at each spliced bar (Fig. 2(b)). The tensile stress f_t required to split those planes is also shown. It is assumed that the tensile stresses are constant across the failure plane.

UNCONFINED BOND MODEL

Considering the two splitting failure modes presented in Fig. 2, a bond model was developed to calculate bond strength. For the sake of simplicity, tensile stresses are assumed to be uniformly distributed along the splice length. Failure is assumed to occur when the entire splice region reaches its tensile capacity. For the side-splitting failure case presented in Fig. 2(a), the force required to cause splitting $F_{splitting}$ can be calculated using the following equation

$$F_{splitting} = \ell_s [2c_{so} + (n-1)2c_{si}] f_t \quad (3)$$

where f_t = concrete tensile strength, psi.

A similar equation can be developed for the face-splitting failure case shown in Fig. 2(b)

$$F_{splitting} = \ell_s (2c_b n) f_t \quad (4)$$

The splitting force is the radial component of the force applied on the concrete by the reinforcing bars. Splitting forces according to Eq. (3) and (4) can be computed using an assumed concrete tensile strength of $6\sqrt{f_c'}$ (psi), where f_c' is the specified compressive strength of concrete (psi). These radial forces are generated by the longitudinal bar forces that can be calculated according to Eq. (5)

$$F_{long} = \sum A_b f_b \quad (5)$$

where f_b = stress on the reinforcing bar, psi.

The radial force $F_{splitting}$ can be related to the longitudinal force F_{long} through the geometrical relationship shown in Fig. 3 and as provided by Eq. (6)

$$\tan\beta = F_{splitting}/F_{long} \quad (6)$$

For a given beam, the angle β can be directly calculated using $F_{splitting}$ and F_{long}. Therefore, β for the 203 unconfined specimens considered was computed. Using this simple model, the average value of angle β for all unconfined data was calculated to be approximately 36 degrees. This value is subsequently considered appropriate for uncoated reinforcing bars. Considering that a value of β is known, the steel stress at splitting failure can easily be calculated using Eq. (5) and (6)

$$f_b = \frac{F_{splitting}}{\sum A_b \tan\beta} \quad (7)$$

The steel stresses from all tests were calculated using a cracked-section analysis. The experimental data was then

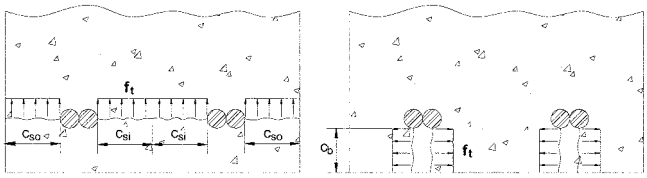

Fig. 2—Physical model of splitting failures.

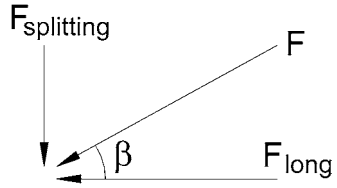

Fig. 3—Relationship between longitudinal and splitting forces.

Table 2—References for confined uncoated splice test data

Reference	Number of tests	Splice length ℓ_s, in.	Bar diameter d_b, in.	Concrete compressive strength f_c', ksi	Concrete cover c, in.
Ferguson and Breen (1965)	9	30.0 to 49.5	1.000 to 1.410	1.82 to 4.17	1.47 to 4.62
Ferguson and Krishnaswamy (1971)	2	30.0 to 54.0	1.693	3.02 to 3.35	2.38 to 3.42
Thompson et al. (1975)	4	15.0 to 30.0	1.000 to 1.410	3.06 to 3.51	2.00
DeVries, Moehle, and Hester (1991)	10	9.0 to 22.0	0.750 to 1.128	7.46 to 16.10	1.06 to 2.44
Rezansoff, Konkankar, and Fu (1992)	34	15.1 to 38.0	0.768 to 1.406	3.28 to 5.74	1.00 to 2.53
Hester et al. (1993)	10	16.0 to 22.8	1.000	5.24 to 6.02	1.50 to 4.00
Rezansoff, Akanni, and Sparling (1993)	11	11.8 to 44.3	0.992 to 1.177	3.63 to 4.09	0.52 to 2.01
Hwang, Lee, and Lee (1994)	4	11.8	1.130	9.01 to 11.68	1.13 to 1.14
Kadoriku (1994)	34	15.0 to 37.4	0.748	3.07 to 10.98	1.12 to 4.80
Darwin et al. (1996)	60	10.0 to 40.0	0.625 to 1.410	3.81 to 5.25	0.40 to 4.50
Hasan, Cleary, and Ramirez (1996)	2	12.0 to 28.0	0.875 to 1.410	3.80 to 3.90	2.38 to 4.63
Hamad and Machaka (1999)	9	12.0	0.984	7.46 to 14.27	1.02 to 1.10
Azizinamini et al. (1999)	25	15.0 to 45.0	1.000 to 1.410	14.58 to 16.00	0.18 to 3.36
Zuo and Darwin (2000)	64	16.0 to 40.0	1.000 to 1.410	4.25 to 15.65	0.40 to 4.03
Total	**278**	**9.0 to 54.0**	**0.625 to 1.693**	**1.82 to 16.10**	**0.18 to 4.80**

compared with the calculated values from Eq. (7) using the average β angle equal to 36 degrees. In this expression, the splitting force was taken as the lower value among the side and face-splitting failure modes. Because the formulation for lap splices in the ACI Code is based on the Orangun, Jirsa, and Breen expression, the results of the proposed expression were compared with the results from this equation. As previously presented in Eq. (1), the Orangun, Jirsa, and Breen expression calculates the average bond stress at failure. This bond stress was used to calculate the bar force and resulting steel stress as given by Eq. (8) so that comparisons could be made

$$f_b = \frac{4\ell_s u}{d_b} \tag{8}$$

It should be noted that the ACI Code equations were not used to compare the performance of the proposed expression. The code equations are design expressions and are not appropriate for the prediction of behavior.

Figure 4 presents the comparison of 203 test results for unconfined, uncoated, and bottom-cast steel bars subjected to a constant moment throughout their splice length. The horizontal axis shows the measured divided by calculated steel stresses, whereas the vertical axis shows the number of occurrences between particular test/calculation ratios. As can be seen from this figure, Eq. (7) performs reasonably well and provides estimates with approximately the same accuracy as the Orangun, Jirsa, and Breen equation.

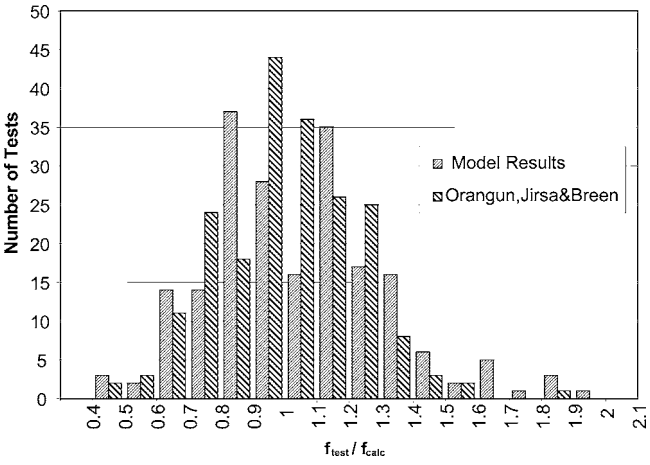

Fig. 4—Comparison of Eq. (1) and (6) for 203 unconfined test data.

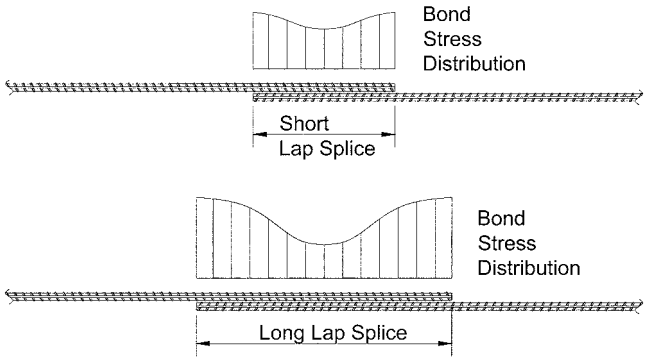

Fig. 5—Assumed bond stress distribution over splice length.

EFFECT OF VARIABLES

Based on this review, it was evident that the simple model provides reasonable estimates of bond strength. The model, however, considers a uniform tensile stress distribution across the entire failure plane. Therefore, it was desirable to investigate the effect of the primary variables that affect this stress distribution as well as the concrete tensile strength to determine if improved results were possible. To isolate the effect of each variable, all variables except the one being investigated were held constant, and test specimens that satisfied the specified conditions were evaluated. As a result of this in-depth examination of the specimens contained in the database, the following variables were found to significantly affect splice behavior.

Splice length

Based on the literature survey, there is an obvious relationship between splice strength and splice length. Previous research has clearly shown that this relationship is not linear (Chinn, Ferguson, and Thompson 1955; Ferguson and Breen 1965; Ferguson and Krishnaswamy 1971). Test results indicate that doubling the splice length does not double the splice strength. Although it was preliminary assumed in Eq. (7) for the sake of simplicity that bond stress is constant over the splice length, a variation can be attributed to the bond stress distribution as shown in Fig. 5. This variation can also be considered as a variation in the tensile stress distribution. As the length of the splice increases, the effectiveness of the splice length decreases; therefore, the relative stress gain reduces. If the splice length is short, the assumption of a constant bond stress distribution (or tensile stress distribution) is fairly accurate. With increasing splice length, however, this assumption becomes less valid, and the accuracy of the calculation drops dramatically.

The database was examined to identify this relationship. First, examination of the database indicated that splice strength is approximately proportional to the square root of the splice length. Second, this relationship is effective considering the ratio of splice length to bar diameter. While a given splice length may be considered long for bars with small diameters, it may be considered short for bars with large diameters. Therefore, splice length is relative. Figure 6 illustrates the effect of the ℓ_s/d_b ratio on bar stress. As shown, all other variables are held approximately constant. Approximations are shown because small variations of the variable were considered acceptable. Also shown are $\alpha\sqrt{\ell_s/d_b}$ curves that were used to best fit the experimental data by changing the multiplier α. These curves show that the square root of the ℓ_s/d_b ratio represents the trend of the experimental data fairly well.

Concrete strength

The concrete strength is incorporated in the model through the use of the tensile strength of concrete $f_t = 6\sqrt{f_c'}$. Because very few test points are available with the concrete strength as the only variable, the experimental steel stress was normalized to provide additional data. The experimental stresses were multiplied by $4.8/\sqrt{\ell_s/d_b}$ based on the analysis previously discussed regarding splice length. This modification factor will be discussed in more detail in a following section. In Fig. 7, the square root and fourth root were compared as noted by the dashed and solid lines. It is apparent that the use of the fourth root of concrete strength instead of the second root fits the test data with improved accuracy. This trend has

also been identified previously by Darwin et al. (1996a,b) and ACI Committee 408 (2003). Additional analyses of the test data indicated that the net effect of the concrete strength is most accurately reflected through the use of the fourth root.

Concrete cover

The effect of cover is linearly incorporated in Eq. (3) and (4). This relation, however, is not linear, and the data shows that as the cover increases, the efficiency reduces. This behavior was expected as the distribution of the tensile stresses on the surrounding concrete of the spliced bar is not constant, but changes as shown in Fig. 1(d). This effect is similar to that presented for the splice length.

Based on analysis of the data, it was evident, much like the splice length, that the c/d_b ratio was important. The effect of the bar diameter can be explained considering the pipe analogy. As the inner diameter of the concrete pipe increases (bar size increases) for a constant wall thickness (cover), the relative thickness of the wall of the pipe decreases. Figure 8 shows the effect of the ratio of concrete cover to bar diameter for side clear cover c_{so}, half of the clear spacing between bars c_{si}, and bottom clear cover c_b. The trend of the data is plotted using the square root of the c/d_b ratio. Experimental steel stresses are normalized with respect to both splice length and concrete strength to enable evaluation, as systematic testing for the effect of the cover has not been conducted. For c_{so}/d_b and c_{si}/d_b curves, only side-splitting

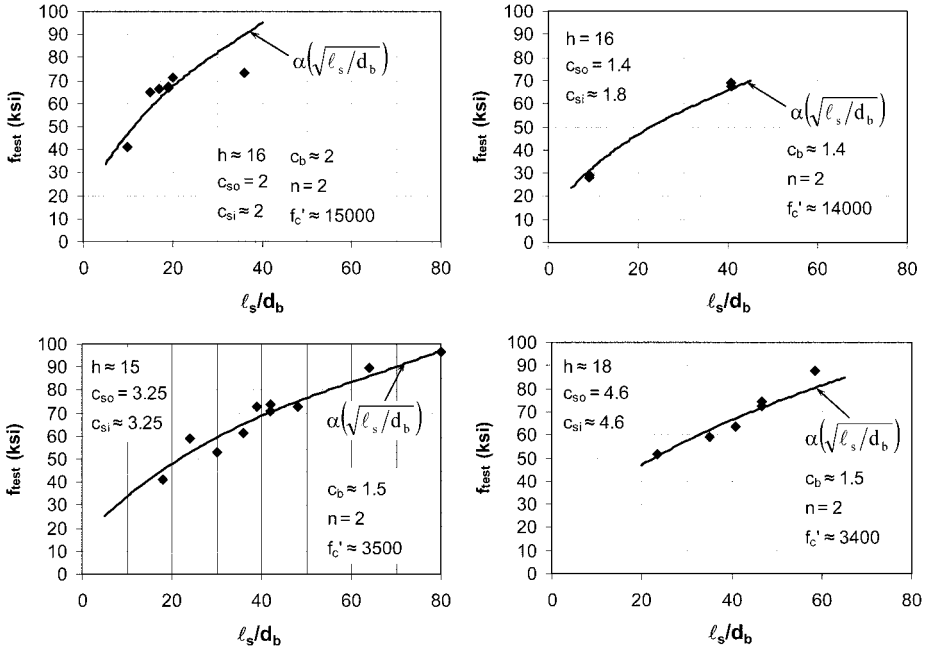

Fig. 6—Effect of splice length.

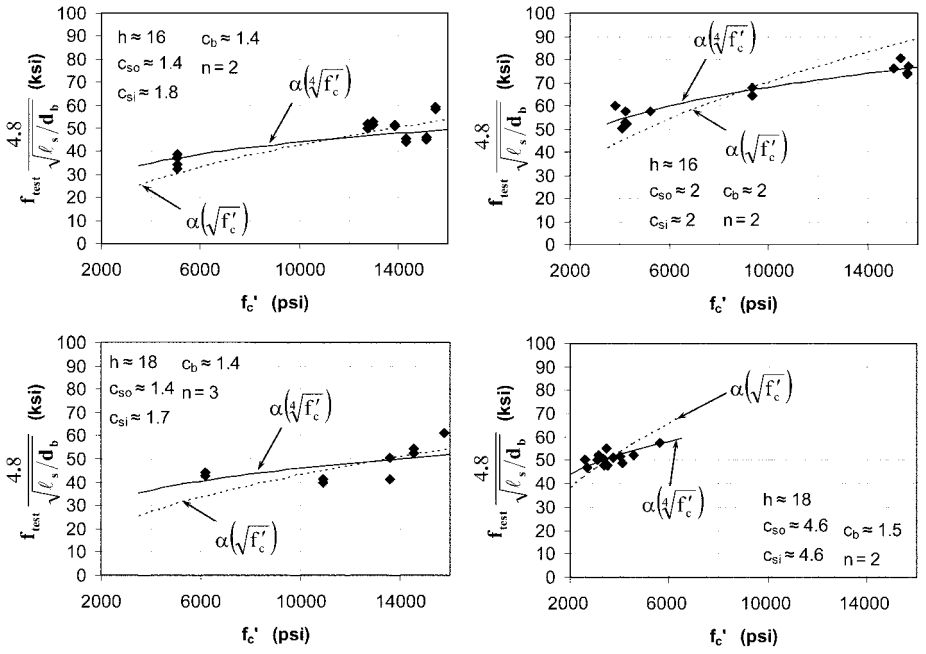

Fig. 7—Effect of concrete strength.

failure data are considered. For c_b/d_b curves, only face-splitting failure data are considered. It was concluded from examination of the database and Fig. 8 that the effective cover thickness can be related to the square root of the cover thickness-to-diameter of the spliced bar ratio $\sqrt{c/d_b}$. This relationship is similar to that noted for splice length.

Inclination of cracks

For face-splitting failures, cracks are assumed vertical as shown in Fig. 2(b). As Orangun, Jirsa, and Breen (1977) stated previously, however, cracks are often V-shaped (Fig. 9). The inclination of the crack increases the splitting length and, accordingly, the total amount of force required for failure. Figure 10 shows the effect of the ratio of side clear cover to face clear cover, c_{so}/c_b, and the ratio of half clear spacing between spliced bars to face clear cover, c_{si}/c_b. Experimental steel stresses are normalized with respect to splice length, concrete strength, and concrete cover. This figure includes only test results from specimens that failed due to face splitting. Evaluation of the test data and Fig. 10 indicate that the increase due to large side concrete cover can be linearly related to the ratio of side cover to face cover, c_{so}/c_b, for the outer cracks and to the ratio of the bar spacing to face cover, c_{si}/c_b, for the inner cracks. The linear trend, as shown in Fig. 10, is $\alpha(0.1c_s/c_b + 0.9)$.

ANALYSIS METHOD

By incorporating the effect of the variables as determined from the detailed analysis, it is possible to obtain a considerably improved estimate of bond strength. The results of this analysis can be incorporated into the model previously presented as follows.

1. Calculate the effective cover. The effective cover can be considered as an equivalent cover dimension where a uniform tensile stress distribution exists

$$c_b^* = c_b \frac{0.77}{\sqrt{c_b/d_b}},\ c_{so}^* = c_{so}\frac{0.77}{\sqrt{c_{so}/d_b}},\ c_{si}^* = c_{si}\frac{0.77}{\sqrt{c_{si}/d_b}} \quad (9)$$

$$\text{where} \quad \frac{0.77}{\sqrt{c/d_b}} \le 1.0$$

2. Calculate effective length. The effective length can be considered as the equivalent splice length where a uniform tensile stress distribution exists

$$\ell_s^* = \ell_s \frac{33}{\sqrt{\ell_s/d_b}\sqrt[4]{f_c'}} \quad (10)$$

$$\text{where} \quad \frac{33}{\sqrt{\ell_s/d_b}\sqrt[4]{f_c'}} \le 1.0$$

3. Calculate the splitting force using Eq. (3) and (4). For these equations, the effective cover and effective length

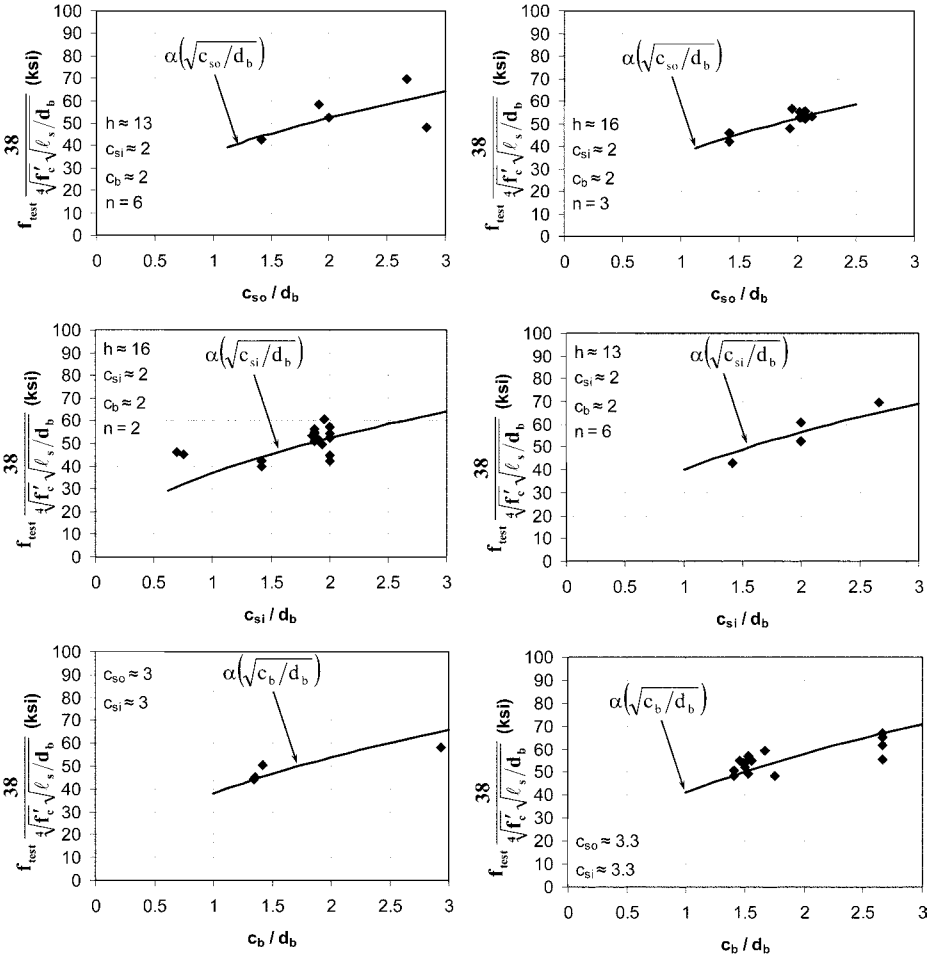

Fig. 8—Effect of concrete cover.

computed previously and $6\sqrt{f_c'}$ for the tensile strength of concrete should be used. In addition, the effect of the crack inclination on face splitting can be included.

Side-splitting failure—

$$F_{splitting} = \ell_s^* [2c_{so}^* + (n-1)2c_{si}^*]6\sqrt{f_c'} \quad (11)$$

Face-splitting failure—

$$F_{splitting} = \ell_s^* \left[2c_b^* \left(0.1\frac{c_{so}}{c_b} + 0.9\right) + 2c_b^* (n-1)\left(0.1\frac{c_{si}}{c_b} + 0.9\right)\right]6\sqrt{f_c'} \quad (12)$$

where $\left(0.1\frac{c_s}{c_b} + 0.9\right) \geq 1.0$

4. Calculate the steel stress assuming β equal to 20 degrees. Previously, this angle was calculated as 36 degrees. After the modification based on the effects of the variables outlined, however, the angle β was reanalyzed. The use of a 20-degree angle was determined to provide optimal results. In this calculation, the lower splitting force from side or face splitting should be used

$$f_b = \frac{F_{splitting}}{nA_b \tan\beta} \quad (13)$$

Modification of cover thickness in Eq. (9) is based on the ratio of cover thickness to diameter of the bar. Figure 11 presents the variation of this modification factor for various c/d_b ratios. The term c represents clear side or face cover or one half of the clear spacing between bars. For a c/d_b ratio of 1.0, the modification factor is 0.77. For wide beams with a c/d_b ratio of 3.0, the factor is 0.44, indicating that only 44% of the cover will be effective. The modification factor for effective cover has a maximum value of 1.0. As shown in Fig. 11, the practical minimum c/d_b ratio according to ACI Code cover limitations is 0.5, considering that the clear spacing between bars should not be taken less than 1.0 in.

Modification of splice length in Eq. (10) is based on the concrete strength and the ratio of splice length to bar diameter. The variation of the splice length modification factor for various concrete strengths is shown in Fig. 12. As noted, the practical minimum limit of the ℓ_s/d_b ratio is 16. This limit is based on ACI 318 Eq. (12-1) considering No. 6 bars, 60 ksi reinforcement, 10,000 psi concrete, 2.5 for confinement factor

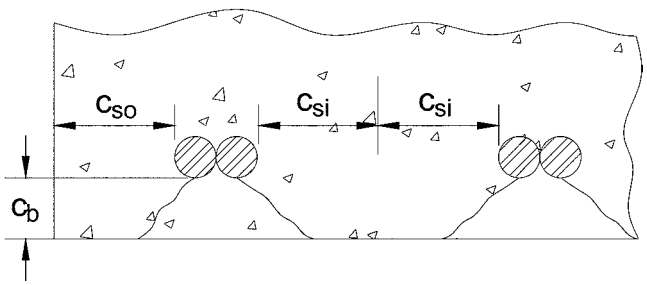

Fig. 9—Assumed crack inclination for face of beam.

(maximum value), and a minimum splice length of 12 in. For normal-strength concrete (4000 psi) and ℓ_s/d_b equal to 16, the coefficient is almost 1.0. For high-strength concrete (10,000 psi), the effective length decreases approximately 20% compared with normal-strength concrete (4000 psi). According to the splice length multiplier, the relationship between bond strength and splice length is not linear; rather, it is related to the square root. Therefore, doubling the splice length, while all other parameters remain constant, increases the bond strength by only 41%.

As discussed previously, for a face-splitting failure, the assumption of vertical cracks over the spliced bars is not accurate. These cracks follow an inclined plane; therefore, the length of the splitting plane will increase. The trend of this modification is shown in Fig. 13. As an example, if the c_s/c_b ratio is 3, the length of the splitting plane will increase

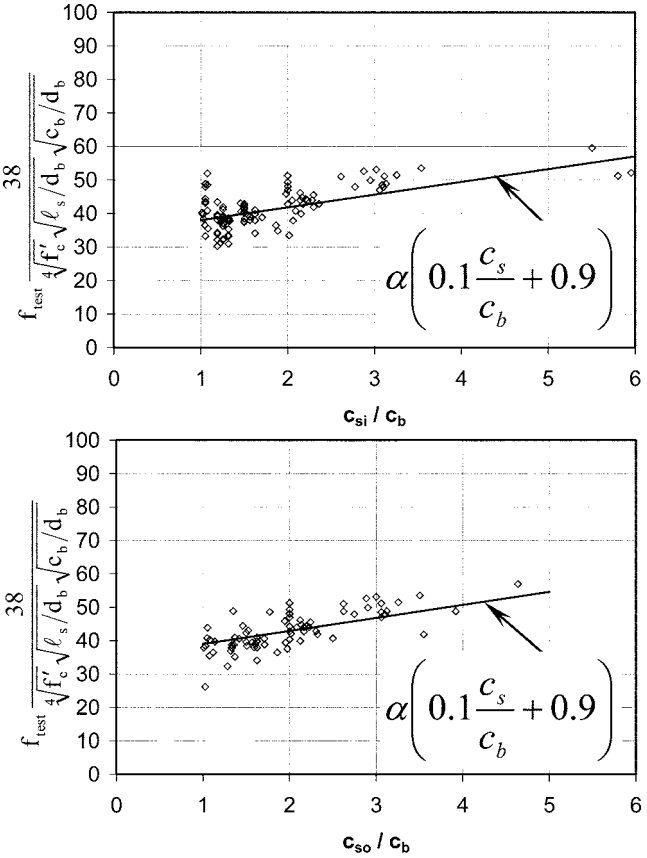

Fig. 10—Effect of ratio of c_{so}/c_b *and* c_{si}/c_b.

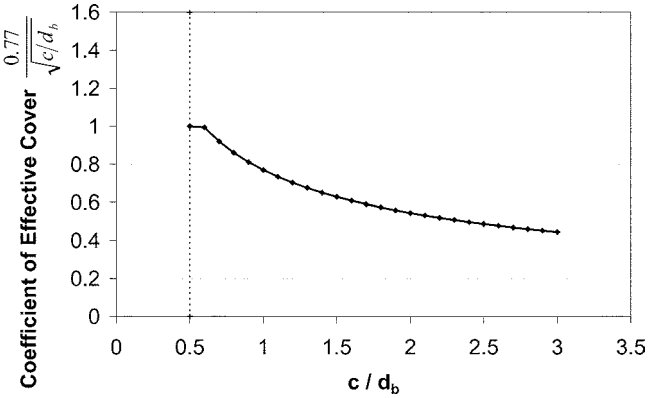

Fig. 11—Variation of coefficient of effective cover.

approximately 20% due to the inclination of the cracks. Accordingly, the bond strength will increase by the same ratio.

To investigate the validity of the modification of the aforementioned variables, the detailed analysis expression was compared with Orangun, Jirsa, and Breen's formulation using the unconfined test data and is shown in Fig. 14. In this figure, calculation according to the expression by Zuo and Darwin (2000) is also provided.

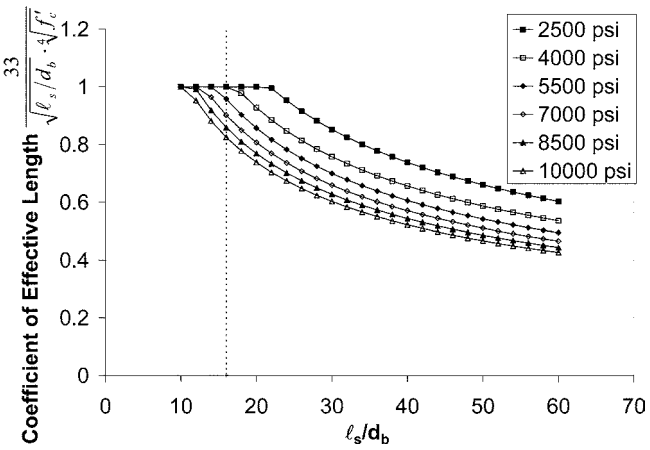

Fig. 12—Variation of coefficient of splice length.

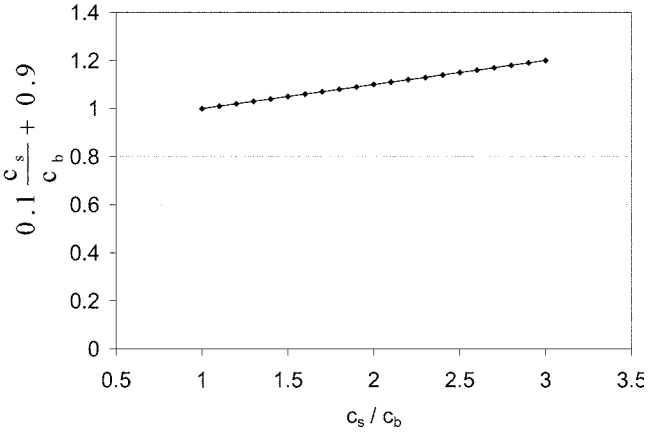

Fig. 13—Variation of coefficient for inclination of cracks in face-splitting failure.

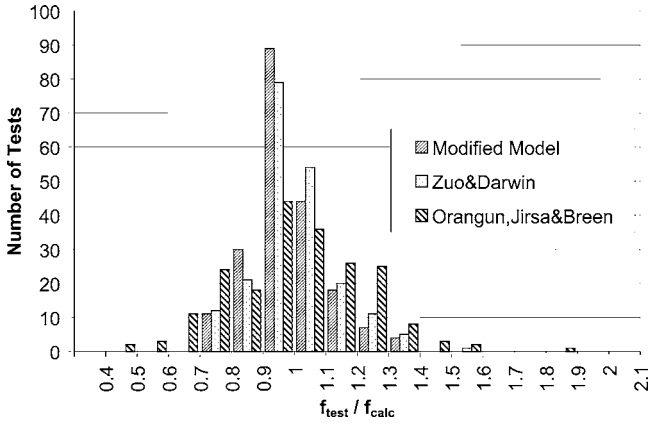

Fig. 14—Comparison of modified analytical expressions for unconfined test data.

Table 3 compares the average, standard deviation, and the product moment coefficient of correlation r^2 of the three expressions. The r^2 indicates how closely the estimated values for the trendline correspond to the actual data. A trendline is most reliable when its r^2 is at or near 1. As indicated by both Table 3 and Fig. 14, the new approach also provides a reasonably accurate method for the calculation of the bond strength of lapped splices.

EFFECT OF CONFINEMENT

Up to this point, only unconfined test results have been considered. The effect of confinement can also be easily incorporated through the addition of a stirrup force to Eq. (13) as shown by Eq. (14). The stirrup provides additional tension resistance across the splitting plane

$$f_b = \frac{F_{splitting} + F_{stirrup}}{nA_b \tan\beta} \tag{14}$$

Force carried by a stirrup can be calculated by multiplying the total area of stirrups crossing the potential failure plane by the stirrup stress. Figure 15 shows the assumed crack plane for the calculation of stirrup force for both side and face splitting.

For the side-splitting case, the horizontal cracking plane is crossed in total by the number of stirrup legs. Therefore, the additional force on the failure plane created by stirrups can be formulated as follows

$$F_{stirrup} = \sum A_{stirrup}\sigma_{stirrup} = N_{st}N_{\ell}A_{st}\sigma_{st} \tag{15}$$

where N_{st} = number of stirrups within the splice length; N_{ℓ} = number of stirrup legs; A_{st} = area of stirrups, in.^{2}; and σ_{st} = stress of stirrups, psi.

As shown in Fig. 15, an orthogonal crack is assumed for face splitting. For simplicity, these face cracks are assumed to be vertical. Because the cracks are close to each other, the reinforcement stress on either side of the two cracks is expected to be approximately the same due to the lack of bond transfer that can occur in the short length between cracks. In other words, the concrete between the cracks is

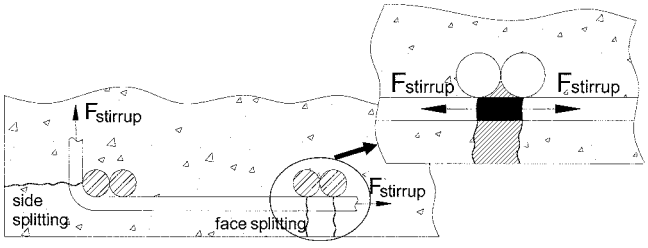

Fig. 15—Assumed crack planes for calculation of stirrup forces.

Table 3—Comparison of expressions for unconfined data

	Average	Standard deviation	r^2
Orangun, Jirsa, and Breen	1.005	0.215	0.567
Zuo and Darwin	1.005	0.128	0.792
Proposed model	0.980	0.118	0.803

considered ineffective. Therefore, the force in the stirrup should only be considered once in this region as it provides tensile resistance across the face cracks as shown. Accordingly, the force developed by the stirrups can be formulated as follows

$$F_{stirrup} = N_{st} n A_{st} \sigma_{st} \quad (16)$$

To calculate the forces developed in the stirrups, the stirrup stress should be known. Similar to the nonuniform tensile stress distribution of concrete over the splice region, the distribution of stress in stirrups over the splice region is nonuniform (Azizinamini, Chisala, and Ghosh 1995; Azizinamini et al. 1999). For the sake of simplicity, however, an analysis was performed using the bond database to calculate an average stirrup stress. Equation (14) was solved for the stirrup force $F_{stirrup}$ using the experimental steel stress f_b and the analytically calculated splitting force $F_{splitting}$. Depending on the splitting mode (side or face), the average steel stress was calculated using Eq. (15) or (16) to be approximately 9000 psi.

The validity of the proposed expression including the effect of confinement is examined in Fig. 16. This figure also includes evaluations performed with expressions suggested by Orangun, Jirsa, and Breen (1977) and Zuo and Darwin (2000). As shown, the new expression reasonably models the effect of confinement on bond. It should be noted that the analysis did not place a limit on the amount of transverse reinforcement considered. For even heavily confined specimens, the use of an average stirrup stress of 9 ksi was found to be appropriate.

To improve the accuracy of the new expression with test results of the confined database, an extensive analysis was performed. All parameters were studied in detail to provide improved modeling for the effect of confinement. In general, it is difficult to isolate variables evaluating confinement. Significant scatter in transverse reinforcement stress was observed when only a limited number of stirrups crossed the plane of splitting. This scatter may be caused by the location of the transverse reinforcement along the splice length because variation is expected in the tensile strain distribution along this length. As the number of stirrups crossing the splitting plane increased, however, the scatter decreased significantly. Through this detailed evaluation, it was found that the following adjustments could be made to the stirrup force as indicated in Eq. (17)

$$\text{Side splitting: } F_{stirrup} = N_{st} N_{\ell} A_{st} \sigma_{st} \left[\frac{\sqrt{f_c'}\, n}{170} \right] \quad (17a)$$

$$\text{Face splitting: } F_{stirrup} = N_{st} n A_{st} \sigma_{st} \left[\frac{\sqrt{f_c'}\, n}{170} \right] \quad (17b)$$

Table 4 presents the average, standard deviation, and r^2 of the various models for the confined case. Both results of the unmodified and modified expressions of the proposed model for the confined case are presented. As noted, modification of the stirrup force slightly improves the statistical values. This improvement can also be observed graphically in Fig. 17. While some improvement in comparisons of measured-versus-calculated results, modification of Eq. (15) and (16) does not significantly improve the results and can be neglected to simplify calculations.

Table 4—Comparison of expressions for confined data

	Average	Standard deviation	r^2
Orangun, Jirsa, and Breen	1.060	0.238	0.465
Zuo and Darwin	0.960	0.125	0.673
Proposed model, unmodified	0.999	0.177	0.565
Proposed model, modified	0.977	0.149	0.636

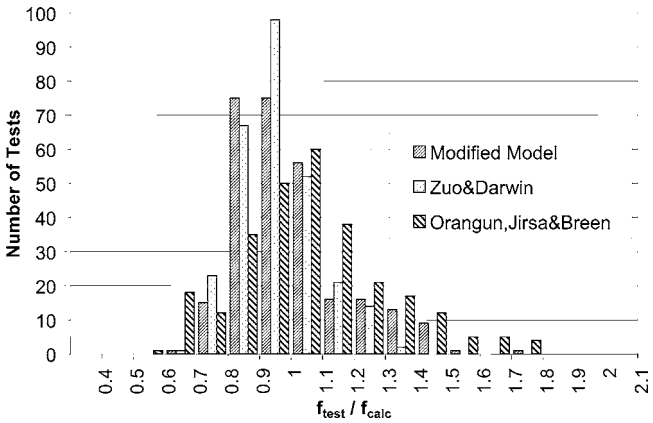

Fig. 16—Comparison of proposed expression for confined case.

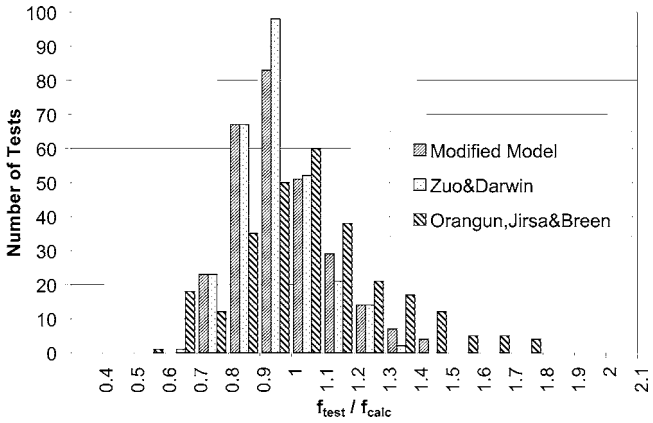

Fig. 17—Comparison of modified expression for confined case.

SUMMARY AND CONCLUSIONS

Test results from 481 beam specimens subjected to constant moment over the splice region were evaluated. Of these specimens, 203 specimens were constructed without transverse reinforcement, while 278 specimens were constructed with transverse reinforcement. Examination and analysis of the database provided the following conclusions:

1. The relation between splice strength and splice length is not linear. It can be expressed approximately by the square root of the ratio of splice length to bar diameter $\sqrt{\ell_s / d_b}$;

2. The use of the fourth root of the concrete strength $\sqrt[4]{f_c'}$ provides an improved estimate regarding the behavior of lapped splices as compared with the square root. This finding is in agreement with the current viewpoint of ACI Committee 408 (2003);

3. The effect of the thickness of the concrete cover surrounding the bar is not linear. The decreasing impact of larger covers can be incorporated by the square root of the cover to bar diameter ratio $\sqrt{c / d_b}$;

4. For face-splitting failure, especially for slab-type members, there is a positive effect of large bar spacing. This trend can be represented by a linear increase in bond strength;

5. Although the strain distribution over the splice region is nonuniform, for sake of simplicity, an average stirrup stress can be considered over the splice region. This stress is independent of the yield strength of the stirrups; and

6. Improved modeling for the effect of confinement can be provided by adjusting the proposed stirrup force by the product of the square root of concrete strength and the number of spliced bars $\sqrt{f_c'}n$. This modification, however, does not significantly improve the results, and can readily be neglected.

Based on the analysis performed, a physical model was developed to calculate the bond strength of reinforced concrete tension lap splices. The model incorporates a nonlinear tensile stress distribution across the splitting plane based on the conclusions presented previously as developed from experimental evidence. The applicability of this expression is supported by evaluation of existing test data that indicates that it reasonably estimates the experimental results of both unconfined and confined test specimens.

CONVERSION FACTORS

1 in. = 25.4 mm
1 kip = 4.448 kN
1 ksi = 6.895 MPa

ACKNOWLEDGMENTS

Erdem Canbay conducted this research as a Postdoctoral Research Associate in the School of Civil Engineering at Purdue University through a grant provided by the NATO Science Fellowship program administered by the Scientific Technical Research Council of Turkey (NATO-B1). Thanks are extended for their support that made this research possible.

REFERENCES

ACI Committee 318, 2002, "Building Code Requirements for Structural Concrete (ACI 318-02) and Commentary (318R-02)," American Concrete Institute, Farmington Hills, Mich., 443 pp.

ACI Committee 408, 1990, "Suggested Development, Splice, and Standard Hook Provisions for Deformed Bars in Tension (ACI 408.1R-90)," American Concrete Institute, Farmington Hills, Mich., 3 pp.

ACI Committee 408, 2003, "Bond and Development of Straight Reinforcing Bars in Tension (ACI 408R-03)," American Concrete Institute, Farmington Hills, Mich., 49 pp.

Azizinamini, A.; Chisala, M.; and Ghosh, S. K., 1995, "Tension Development Length of Reinforcing Bars Embedded in High-Strength Concrete," *Engineering Structures*, V. 17, No. 7, pp. 512-522.

Azizinamini, A.; Pavel, R.; Hatfield, E.; and Ghosh, S. K., 1999, "Behavior of Lap-Spliced Reinforcing Bars Embedded in High-Strength Concrete," *ACI Structural Journal*, V. 96, No. 5, Sept.-Oct., pp. 826-835.

Azizinamini, A.; Stark, M.; Roller, J. J.; and Ghosh, S. K., 1993, "Bond Performance of Reinforcing Bars Embedded in High-Strength Concrete," *ACI Structural Journal*, V. 90, No. 5, Sept.-Oct., pp. 554-561.

Chamberlin, S. J., 1958, "Spacing of Spliced Bars in Beams,"ACI JOURNAL, *Proceedings* V. 54, No. 2, Feb., pp. 689-697.

Chinn, J.; Ferguson, P. M.; and Thompson, J. N., 1955, "Lapped Splices in Reinforced Concrete Beams," ACI JOURNAL, *Proceedings* V. 52, No. 10, Oct., pp. 201-213.

Choi, O. C.; Hadje-Ghaffari, H.; Darwin, D.; and McCabe S. L., 1991, "Bond of Epoxy-Coated Reinforcement: Bar Parameters," *ACI Materials Journal*, V. 88, No. 2, Mar.-Apr., pp. 207-217.

Cleary, D. B., and Ramirez, J. A., 1991, "Bond Strength of Epoxy-Coated Reinforcement," *ACI Structural Journal*, V. 88, No. 2, Mar.-Apr., pp. 146-149.

Darwin, D.; Tholen, M. L.; Idun, E. K.; and Zuo, J., 1996a, "Splice Strength of High Relative Rib Area Reinforcing Bars," *ACI Structural Journal*, V. 93, No. 1, Jan.-Feb., pp. 95-107.

Darwin, D.; Zuo, J.; Tholen, M. L.; and Idun, E. K., 1996b, "Development Length Criteria for Conventional and High Relative Rib Area Reinforcing Bars," *ACI Structural Journal*, V. 93, No. 3, May-June, pp. 347-359.

DeVries, R. A.; Moehle, J. P.; and Hester, W., 1991, "Lap Splice Strength of Plain and Epoxy-Coated Reinforcements: An Experimental Study Considering Concrete Strength, Casting Position, and Anti-Bleeding Additives," *Report* No. UCB/SEMM-91/02, Department of Civil Engineering, University of California Berkeley, Berkeley, Calif., Jan., 93 pp.

Ferguson, P. M., and Breen, J. E., 1965, "Lapped Splices for High Strength Reinforcing Bars, Part I & II," ACI JOURNAL, *Proceedings* V. 62, Sept., pp. 1063-1077.

Ferguson, P. M., and Briceno, E. A., 1969, "Tensile Lap Splices—Part I: Retaining Wall Type, Varying Moment Zone," *Research Report* No. 113-2, Center for Highway Research, The University of Texas at Austin, Austin, Tex., July, 39 pp.

Ferguson, P. M., and Krishnaswamy, C. N., 1971, "Tensile Lap Splices—Part 2: Design Recommendation for Retaining Wall Splices and Large Bar Splices," *Research Report* No. 113-2, Center for Highway Research, The University of Texas at Austin, Austin, Tex., Apr., 60 pp.

Goto, Y., 1971, "Cracks Formed in Concrete around Deformed Tension Bars," ACI JOURNAL, *Proceedings* V. 68, No. 4, Apr., pp. 244-251.

Hamad, B. S., and Itani, M. S., 1998, "Bond Strength of Reinforcement in High-Performance Concrete: The Role of Silica Fume, Casting Position, and Superplasticizer Dosage," *ACI Materials Journal*, V. 95, No. 5, Sept.-Oct., pp. 499-511.

Hamad, B. S., and Machaka, M. F., 1999, "Effect of Transverse Reinforcement on Bond Strength of Reinforcing Bars in Silica Fume Concrete," *Materials and Structures*, V. 32, July, pp. 468-476.

Hamad, B., and Mansour, M., 1996, "Bond Strength of Noncontact Tension Lap Splices," *ACI Structural Journal*, V. 93, No. 3, May-June, pp. 316-326.

Hasan, H. O.; Cleary, D. B.; and Ramirez, J. A., 1996, "Performance of Concrete Bridge Decks and Slabs Reinforced with Epoxy-Coated Steel under Repeated Loading," *ACI Structural Journal*, V. 93, No. 4, July-Aug., pp. 397-403.

Hester, C. J.; Salamizavaregh, S.; Darwin, D.; and McCabe, S. L., 1993, "Bond of Epoxy-Coated Reinforcement: Splices," *ACI Structural Journal*, V. 90, No. 1, Jan.-Feb., pp. 89-102.

Hwang, S. J.; Lee, Y. Y.; and Lee, C. S., 1994, "Effect of Silica Fume on the Splice Strength of Deformed Bars of High-Performance Concrete," *ACI Structural Journal*, V. 91, No. 3, May-June, pp. 294-302.

Jirsa, J. O.; Lutz, L. A.; and Gergely, P., 1979, "Rationale for Suggested Development, Splice, and Standard Hook Provisions for Deformed Bars in Tension," *Concrete International*, V. 1, No. 7, July, pp. 47-61.

Kadoriku, J., 1994, "Study on Behavior of Lap Splices in High-Strength Reinforced Concrete Members," doctorate thesis, Kobe University, Japan, Mar., 201 pp.

Orangun, C. O.; Jirsa, J. O.; and Breen, J. E., 1977, "A Reevaluation of Test Data on Development Length and Splices," ACI JOURNAL, *Proceedings* V. 74, No. 3, Mar., pp. 114-122.

Rezansoff, T.; Akanni, A.; and Sparling, B., 1993, "Tensile Lap Splices under Static Loading: A Review of the Proposed ACI 318 Code Provisions," *ACI Structural Journal*, V. 90, No. 4, July-Aug., pp. 374-384.

Rezansoff, T.; Konkankar, U. S.; and Fu, Y. C., 1992, "Confinement Limits for Tension Lap Splices under Static Loading," *Canadian Journal of Civil Engineering*, V. 19, pp. 447-453.

Tepfers, R., 1979, "Cracking of Concrete Cover Along Anchored Deformed Reinforcing Bars," *Magazine of Concrete Research*, V. 31, No. 106, pp. 3-12.

Tepfers, R., 1982, "Lapped Tensile Reinforcement Splices," *Journal of the Structural Division*, ASCE, V. 108, No. ST1, pp. 283-301.

Thompson, M. A.; Jirsa, J. O.; Breen, J. E.; and Meinheit, D. F., 1975, "The Behavior of Multiple Lap Splices in Wide Sections," *Research Report* No. 154-1, Center for Highway Research, The University of Texas at Austin, Austin, Tex., Feb., 75 pp.

Treece, R. A., and Jirsa, J. O., 1989, "Bond Strength of Epoxy-Coated Reinforcing Bars," *ACI Materials Journal*, V. 86, No. 2, Mar.-Apr., pp. 167-174.

Zuo, J., and Darwin, D., 2000, "Splice Strength of Conventional and High Relative Rib Area Bars in Normal and High-Strength Concrete," *ACI Structural Journal*, V. 97, No. 4, July-Aug., pp. 630-641.